Functionalized Graphene Nanoribbons *via* Anionic Polymerization Initiated by Alkali Metal-Intercalated Carbon Nanotubes

Wei Lu,[†] Gedeng Ruan,[†] Bostjan Genorio,[†,‡] Yu Zhu,[†,#] Barbara Novosel,[‡] Zhiwei Peng,[†] and James M. Tour*[,†,§,⊥]

[†]Department of Chemistry, [§]Department of Mechanical Engineering and Materials Science, and [⊥]Richard E. Smalley Institute for Nanoscale Science and Technology, Rice University, 6100 Main Street, Houston, Texas 77005, United States, and [‡]Faculty of Chemistry and Chemical Technology, University of Ljubljana, Aškerčevacesta 5, 1000 Ljubljana, Slovenia. [#]Present address: Department of Polymer Science, The University of Akron, Akron, Ohio 44325—3909.

ABSTRACT The preparation of polymer-functionalized graphene nanoribbons (PF-GNRs) in a one-pot synthesis is described. Multiwalled carbon nanotubes (MWCNTs) were intercalated by potassium under vapor- or liquid-phase conditions, followed by the addition of vinyl or epoxide monomers, resulting in PF-GNRs. Scanning electron microscopy, thermogravimetric mass spectrometry, and X-ray photoelectron spectroscopy were used to characterize the PF-GNRs. Also explored here is the correlation between the splitting of MWCNTs, the intrinsic properties of the intercalants and the degree of defects and graphitization of the starting MWCNTs. The PF-GNRs could have applications in conductive composites, transparent electrodes, heat circuits, and supercapacitors.

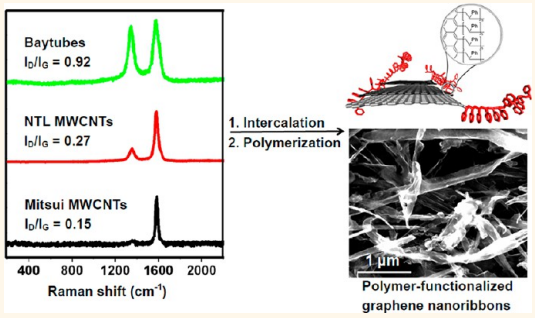

KEYWORDS: graphene nanoribbons · intercalation · graphitization · anionic polymerization · carbon nanotubes

Owing to their interesting electronic and mechanical properties, graphene nanoribbons (GNRs) have attracted attention for use in the preparation of conductive composites, and several techniques have been explored to synthesize bulk quantities of functionalized GNRs.[1] GNRs have been obtained through oxidative unzipping of multiwalled carbon nanotubes (MWCNTs) using potassium permanganate and sulfuric acid,[2] by intercalating lithium into MWCNTs followed by thermal expansion,[3] and by longitudinal splitting of MWCNTs using transition metal clusters.[4] GNRs have also been prepared *via* intercalation of potassium into MWCNTs[5,6] or expansion of MWCNTs using molecular nitrogen.[7] To produce conductive and mechanically reinforced GNR composites, the GNRs must be well-dispersed in the polymer matrix, and to this end, functionalization of the GNRs is critical. However, the existing approaches do not generate bulk quantities of GNRs functionalized with addends that render the products well-dispersible in polymer matrices. Here, we demonstrate that, in analogy to the intercalation chemistry of graphite, potassium intercalation into MWCNTs followed by *in situ* reaction with vinyl or epoxide monomers results in exfoliation of the MWCNTs and subsequent splitting with functionalization into polymer-functionalized GNRs (PF-GNRs) in a one-pot solution-based process. These polymer addends provide enhanced integration between the GNRs and polymer matrices. Furthermore, since polymerization is mainly initiated from GNR edges, the basal planes can remain sp^2-hybridized. This stands in contrast to the covalent functionalization of carbon nanotubes where the functionalized nanotubes must contain sp^3-hybridized carbons at all functionalization sites. We also correlate the exfoliation of MWCNTs with the structural characteristics of the starting materials and the intrinsic properties of the intercalants. This scalable and low-cost approach to functionalized GNRs produces

* Address correspondence to tour@rice.edu.

Received for review January 4, 2013 and accepted February 7, 2013.

Published online February 07, 2013
10.1021/nn400054t

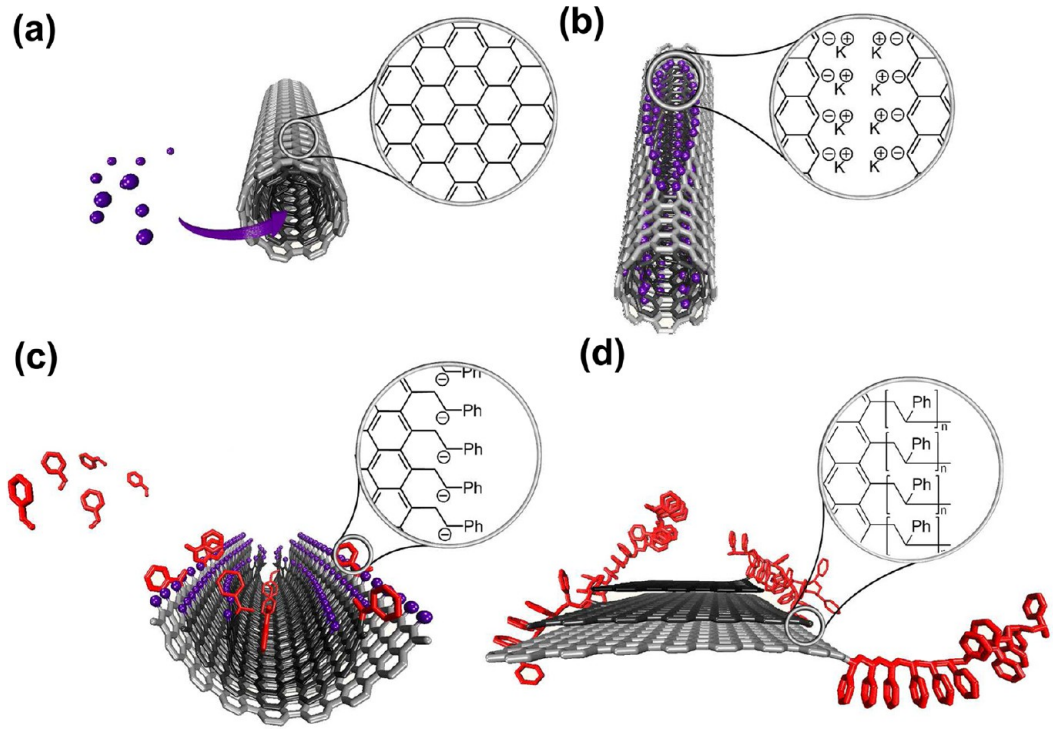

Figure 1. Reaction scheme for the one-pot synthesis of functionalized GNRs. (a) The MWNTs are intercalated with potassium naphthalenide (blue dots). (b) A longitudinal fissure is formed in the walls of the MWCNTs due to expansion caused by intercalation of THF-stabilized potassium ions into the MWCNT host. The edge radicals would be immediately reduced to the corresponding anions under the reducing conditions. (c) Polymerization of styrene (for instance) assists in exfoliation of MWCNTs. (d) PF-GNRs are formed upon quenching.

materials that could be useful for transparent electrodes and heat circuits, electroactive polymer/graphene supercapcitors, and conductive nanocomposites.

RESULTS AND DISCUSSION

The synthetic strategy for the one-pot synthesis of PF-GNRs used in the present study is shown in Figure 1. MWCNTs were converted into edge-negatively charged polymerization macroinitiators *via* intercalation and splitting. It is assumed, based on the proposed mechanism, that the edges of the split tubes are lined by aryl anions and their associated metal cations. Second, anionic polymerization of vinyl monomers starting at the negatively charged GNR edges results in PF-GNRs. An analogous alkylation with alkyl halides was recently disclosed with Na/K.[6] While the vapor phase intercalation of MWCNTs was reported earlier,[5] the potassium naphthalenide liquid-phase intercalation will be described here along with the subsequent polymerization methodology (see the Supporting Information for the detailed synthesis of polystyrene functionalized GNRs through vapor-phase intercalation). Briefly, MWCNTs, potassium metal, naphthalene, and THF were added to a Schlenk flask and subjected to three freeze–pump–thaw cycles to remove oxygen. As suggested by our previous work,[5] the intercalation of solvent-stabilized potassium cations into MWCNTs may lead to expansion of the *d*-space between MWCNT layers, causing the MWCNTs to partially or fully split.[5,6] The fissures in the sidewalls of the MWCNTs serve as the starting points for vinyl or epoxide monomers to anionically polymerize from the GNR edges. Because of polymerization probably proceeding between the GNR layers, only a small amount of olefin was needed to effect the exfoliation of the MWCNTs. The nonattached polymer was removed by extracting the raw product with boiling chloroform in a Soxhlet extractor.

Scanning electron microscopy (SEM) was used to image the MWCNTs after intercalation and polymerization. PF-GNRs with widths in the range of several hundred nanometers are clearly shown in Figure 2 (see Figures S1–S3 in Supporting Information for additional images). These PF-GNRs are able to be suspended in THF far more easily than the proton-edged GNRs (from methanol quenching) owing to the polymer addends (Supporting Information, Figure S2c). This is suggests a likelihood for PF-GNRs to be more easily dispersed in host polymers.

Thermogravimetric mass spectrometry (TG-MS) was used to confirm the presence of the polystyrene chains, to estimate the quantity of the repeat units, and to determine the temperature window of degradation of the PF-GNRs. To exclude the influence of the surface physisorbed components, all of the PF-GNRs were extracted with chloroform in a Soxhlet extractor for 1 week and then dried at 60 °C overnight. The thermogravimetric analysis (TGA) thermogram (Figure 3a)

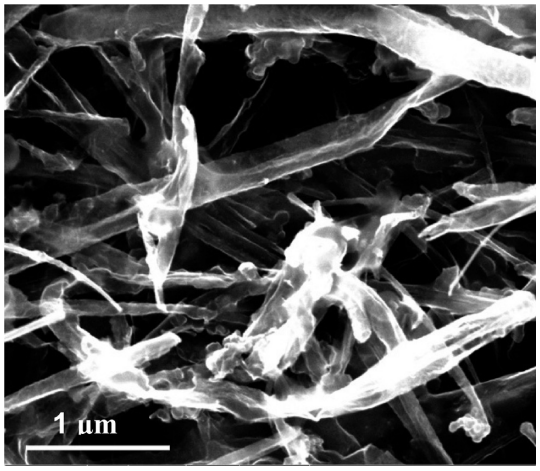

Figure 2. Representative SEM image of MWCNTs treated with potassium naphthalenide followed by the addition of styrene (see Figure S3 in Supporting Information for SEM images of Mitsui MWCNTs treated with potassium naphthalenide followed by the addition of isoprene). GNRs can be readily identified under SEM; their widths are in the range of several hundred nanometers. The amorphous material wrapping the GNRs or extending across neighboring GNRs is polystyrene.

indicates a one-step weight-loss process with a total weight loss of 9% between 100 and 900 °C. Major decomposition occurs between 384 and 474 °C. According to MS analysis and a previous report,[8] this is the range where depolymerization of the polystyrene occurs. Charged molecule fragments with mass to charge ratios (*m/z*) 78, 77, 51, and 50 were observed, with intensities that are distinct for the styrene monomer, one of the expected degradation products.[9] A control experiment with starting MWCNTs was also performed where no weight loss was observed (blue curve in Figure 3a). On the basis of the weight loss between 384 and 474 °C, the weight ratio between the styrene monomer unit and carbon atoms of the graphene material was 1:136. If all of the edge carbons of the graphene nanoribbons were functionalized, this data would indicate that the average polymer chain length was only 9 units for a 3 μm $\times$ 150 nm ribbon (see Supporting Information for the calculation), but it is unlikely that all sites had equal exposures to the monomer, so dramatically varied chain lengths are presumed. However, further definition of this point is not easily obtained, nor is it in the ultimate interest of our study.

Raman spectroscopy was also used to characterize the graphitic structure of the PF-GNRs. An increase in the intensity of the D band over the G band from 0.15 for MWCNTs to 0.35 for PF-GNRs was observed in Figure 3b. Upon splitting of MWCNTs, a prominent D peak is an indication of disorder in the graphene structure due to the high edge content.[5] The disordered structure also results in a slight broadening of the G band[10] and the 2D band,[11] as well as the combination mode of D + G band[12] at ~2700 cm^{-1} in

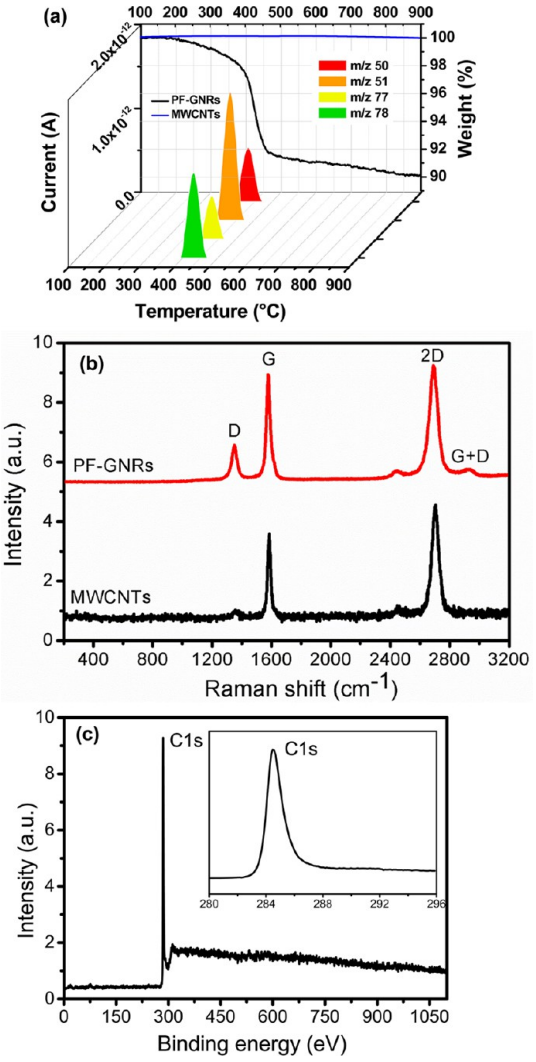

Figure 3. Characteristics of PF-GNRs. (a) 3D TG-MS spectra of the gas phase in the thermal degradation of PF-GNRs and MWCNTs. Different colors represent gas products with different *m/z* in which *m* is the mass of the gas products and *z* is the charge. The black and blue curves correspond to the TGA profile of PF-GNRs and starting MWCNTs, respectively. (b) Raman spectra of PF-GNRs and MWCNTs. (c) XPS survey spectrum of PF-GNRs. The inset is high-resolution XPS C1s spectrum of PF-GNRs, indicating PF-GNRs are nearly free of oxidation.

PF-GNRs. However, a splitting of the G band,[13] corresponding to an intercalated graphitic structure, is not observed in the Raman spectrum, implying that little residual intercalants, if any, or solvents were between the PF-GNRs. X-ray photoelectron spectroscopy (XPS) was used to examine the PF-GNR surface functionalities. The survey spectrum in Figure 3c shows that no oxygen was detected in the PF-GNRs. This is further confirmed by the high-resolution XPS C1s spectrum in the inset of Figure 3c, as no peaks corresponding to 286 eV (C−O) or 287 eV (C═O) were observed.[2]

To further explore polymerization initiated by reactive GNR anions, MWCNTs were potassium vapor-treated at 350 °C for 24 h.[5] The product was transferred to a round-bottom flask in the glovebox and styrene

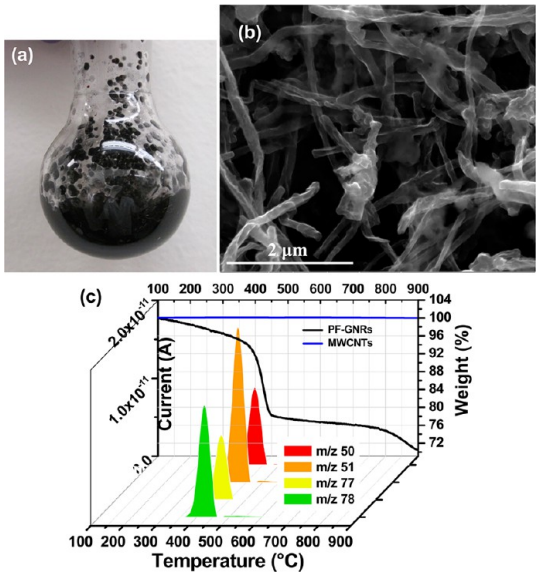

Figure 4. Characteristics of potassium vapor-treated MWCNTs quenched with styrene. (a) Photograph of the polymerization of styrene initiated by potassium-vapor-treated MWCNTs. (b) Representative SEM image of split MWCNTs. The majority of MWCNTs were split and ribbon-like structure could be identified in the image (see Figures S4 in Supporting Information SII for SEM images of Mitsui MWCNTs treated with potassium vapor followed by addition of isoprene). (c) 3D plot of the TG-MS results of PF-GNRs and MWCNTs. Different colors represent gas products with different *m/z*. The black and blue curves correspond to the TGA profile of PF-GNRs and MWCNTs, respectively.

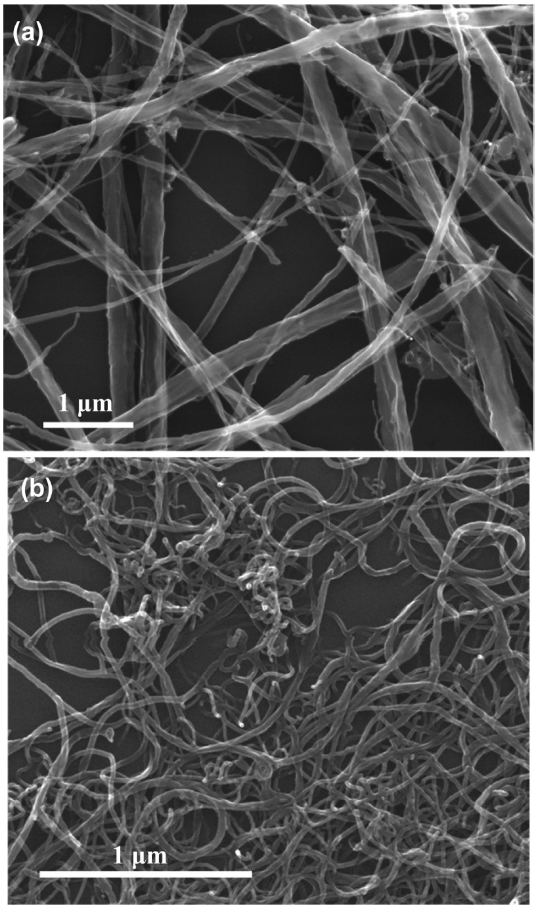

Figure 5. (a) SEM image of NTL MWCNTs treated with potassium naphthalenide in THF followed by addition of styrene. The majority of NTL MWCNTs are split but they are not completely flattened to form ribbon-like structure (see Figure S6 in Supporting Information for SEM images of pristine NTL MWCNTs). (b) SEM image of Baytubes treated with potassium naphthalenide in THF followed by the addition of styrene. Some of the MWCNTs are split due to intercalation followed by polymerization but many others retain their tube-like structure (see Figure S7 in Supporting Information for the SEM image of pristine Baytubes).

was added dropwise. The reaction mixture was kept at room temperature for 24 h and then at 60 °C overnight to complete the polymerization. The potassium intercalated MWCNTs were fluffy and randomly distributed inside the flask. The addition of styrene monomer led to plastic beads with black centers, indicating the growth of polystyrene on partially split GNRs, as shown in Figure 4a (see Supporting Information for the one-pot synthesis protocol). Some ribbon-like structures were identified in Figure 4b (see Figure S4 in Supporting Information for additional images). The TGA in Figure 4c shows that the weight loss was 22% (after extensive Soxhlet extraction with chloroform), four times higher than that of MWCNTs treated in the liquid-phase intercalation process.

To further show that the edge polymerization was not limited to vinyl monomer, ethylene oxide was used to generate poly(ethylene oxide) functionalized GNRs (PEO-GNRs). These showed ~20% PEO content by TGA analysis (Figure S5 in the Supporting Information for the SEM image and TGA data).

To explore the flexibility of the present protocol, two other sources of MWCNTs, NanoTechLabs MWCNTs (NTL MWCNTs) and Bayer MWCNTs (Baytubes), were subjected to the reaction to compare the results to those from the Mitsui MWCNTs used for the former two experiments. Upon liquid-phase intercalation followed by polymerization, NTL MWCNTs were split but not further flattened to form GNRs (Figure 5a). With the Baytubes MWCNTs, although some partially flattened GNRs could be identified, most of the MWCNTs remained intact (Figure 5b).

Generally, the charge transfer from naphthalene radical anions to the graphitic structure is governed by the electronic state of the host material.[14] If the host materials are highly crystalline, overlap of the valence and conduction bands could lead to two carriers, electrons and holes, in the conjugated graphene plane. Therefore, the electrons, during intercalation, can be transferred from the potassium naphthalenide to the host to balance the concentration of holes, and then into the graphene conduction band. Consequently, well-defined graphite intercalation compounds (GICs) can be obtained from highly crystallized hosts. For materials with a low degree of crystallinity, unorganized intercalation structures are observed since there is

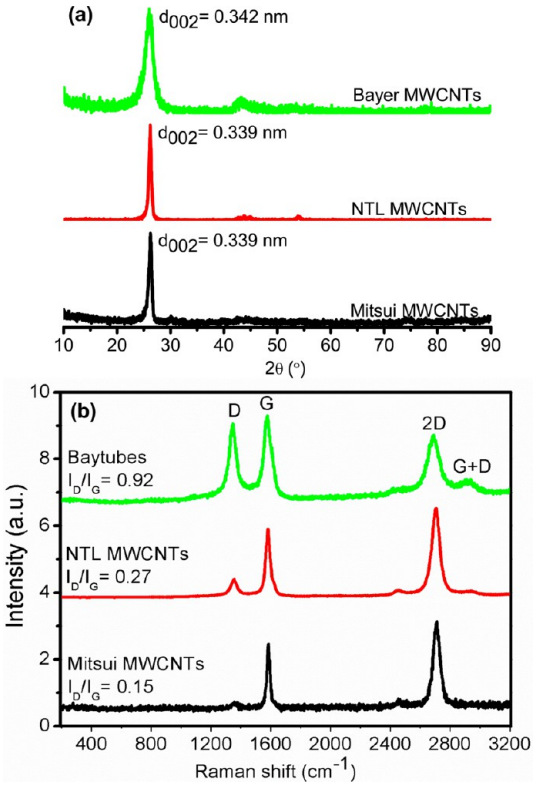

Figure 6. Spectral fingerprints from three different MWCNT sources. (a) XRD patterns of Mitsui MWCNTs, NTL MWCNTs, and Baytubes. The d_{002} was calculated according to Bragg's equation $\lambda = 2d \sin \theta$, where λ is 1.54 Å for Cu Kα. (b) Raman spectra of Mitsui MWCNTs, NTL MWCNTs and Baytubes. Baytubes have the highest I_D/I_G, indicating the most defective graphitic structure. Also present is the combination of G+D band[12] induced by disorder structure, which is not observed in Mitsui MWCNTs or NTL MWCNTs.

no overlap between the conduction band and the valence band due to the disrupted graphitic structures. Previous work on exfoliation of GICs[15,16] suggests that forming a well-defined intercalation structure could be a prerequisite for making exfoliated GNRs *via* polymerization-assisted exfoliation of MWCNTs. The important link between the structural characteristics of the MWCNTs host and splitting and exfoliation of MWCNTs has been less explored, despite the fact that Mordkovich *et al.* studied the scroll carbon nanotubes by intercalating potassium metal into carbon nanotubes.[17] The degree of graphitization can be calculated from the interplanar *d* spacing between two graphitic layers, according to eq 1:[18]

$$g = \frac{0.3440 - d_{002}}{0.3440 - 0.3354} \quad (1)$$

where *g* is the degree of graphitization, 0.3440 (nm) is the interlayer spacing of the fully nongraphitized carbon; 0.3354 (nm) is the *d* spacing of the ideal graphite crystallite and d_{002} (nm) derived from X-ray diffraction (XRD) is the interlayer spacing corresponding to (002) planes of the graphitic material. For Mitsui MWCNTs and NTL MWCNTs, $g = 0.58$, which is higher than that for

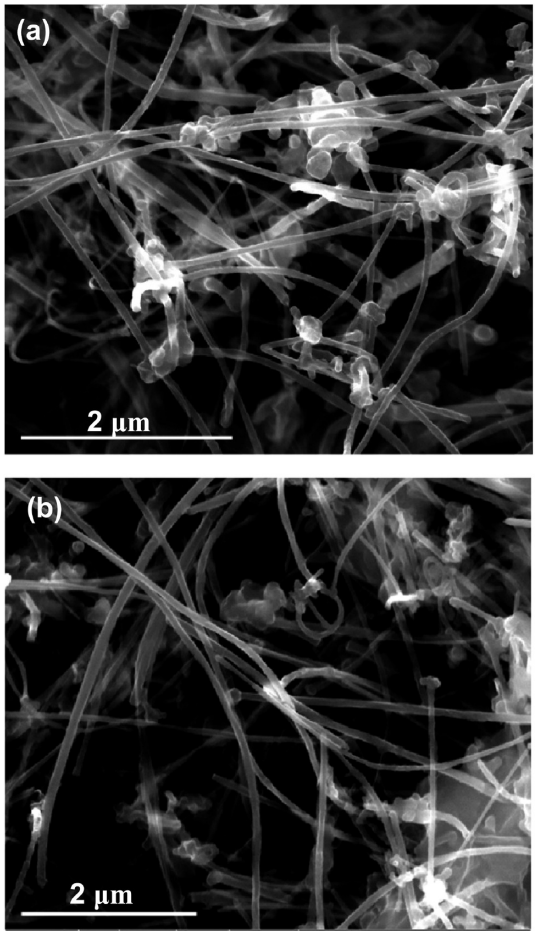

Figure 7. Representative SEM images of styrene-treated alkali-metal intercalated MWCNTs. (a) SEM image of MWCNTs treated with sodium naphthalenide followed by styrene. (b) SEM image of MWCNTs treated with lithium naphthalenide followed by styrene. Clearly, most MWCNTs remained intact in these two cases, because sodium naphthalenide or lithium naphthalenide failed to form fissure structures on MWCNTs for further splitting.

Bayer MWCNTs, where $g = 0.23$ (Figure 6), indicating that more facile exfoliation of the carbon host would be possible with Mitsui and NTL nanotubes. Note that the presence of any disordered structures caused by sp^3-hybridized carbons or defects that could terminate the splitting or exfoliation of MWCNTs cannot be determined from XRD patterns. Consequently, Raman spectroscopy was used to differentiate the degree of disordered structure in the host materials by calculating the ratio of the intensity of the D band to the G band.[19] The relative intensity of disorder-induced D band to crystalline G band, I_D/I_G, is 0.15 for Mitsui MWCNTs, 0.27 for NTL MWCNTs, and 0.92 for Baytubes, as shown in Figure 6b. Defect sites on graphite do not favor the formation of well-defined intercalation structure[14] and thus the complete exfoliation of highly defective Baytubes by intercalation is likely more difficult (Figure S8 in the Supporting Information for TEM images). This is corroborated by recent work on reductive alkylation of MWCNTs with potassium naphthalenide, in which the

outer surface of highly defective MWCNTs ($I_D/I_G > 1$) were functionalized with decanoic acid and no ribbon-like structure was observed in the SEM images.[20] Although NTL MWCNTs have fewer defects, flattening ultralong split tubes may require further treatment. Thus, most NTL MWCNTs remained split and stacked rather than completely flattened (see Figure S9 in the Supporting Information for TEM images). It is difficult to precisely establish the structural threshold (*i.e.*, the critical value for g or I_D/I_G) that can be used to predict if the MWCNTs can be split and exfoliated; however, it is noteworthy that the higher the degree of graphitization of the carbon host, or the less defective the carbon host, the easier the exfoliation of the MWCNTs *via* intercalation.

Similar to the degree of graphitization of the starting carbon nanotubes, the ionization potential and the atomic size of the alkali metals also play an active role in intercalation and subsequent exfoliating. Since sodium naphthalenide and lithium naphthalenide have been used to make GICs[18,21] and they are also commonly used as initiators for anionic polymerization, the intercalation of solvent-stabilized sodium and lithium into MWCNTs for making functionalized GNRs was explored.

However, neither of the reaction products contained significant numbers of exfoliated MWCNTs; most of the MWCNTs remained intact, as shown by the SEM images in Figure 7. Both lithium and sodium failed to form significant fissures on MWCNTs for subsequent exfoliation assisted by polymerization, as discussed in our previous work.[5]

CONCLUSIONS

The wet chemical preparation of high-quality PF-GNRs was achieved by polymerization-assisted exfoliation of MWCNTs in a one-pot synthesis. The *in situ* functionalized GNRs were examined by TG/MS, SEM, TEM, and Raman spectroscopy. Compared to MWCNTs treated with potassium vapor followed by the addition of isoprene, the liquid-phase intercalation of MWCNTs and subsequent polymerization was more efficient in exfoliating MWCNTs to form PF-GNRs, but with less polymer bound onto the edges. Also demonstrated was the correlation between the structural characteristics of the host (the degree of graphitization and the intensity of D band over G band) and the exfoliation efficiency. The PF-GNRs or split tubes could be used for reinforcing polymers, since the sword-in-sheath type failure of MWCNTs due to interlayer slip[22] could be retarded owing to the entangled polymer chains anchored on the edges. Through the compatiblizing appended polymer chains, the load might be effectively transferred from the polymer matrix to the rigid PF-GNRs, thus making stronger composites. In addition, it has been shown that functionalized GNRs remain conductive since the functionalization preferably occurs on the graphene edges.[6] Systematic studies are underway to better understand the correlation between functionalization and conductivity of the PF-GNRs for use in making reinforced conductive composites and conductive transparent films.

METHODS

MWCNTs were obtained from Mitsui & Co. (lot no. 05072001K28), NanoTechLabs, Inc. (lot no. no. 5T10M10), or Bayer MaterialScience (lot no. C720P) and they were used as received. THF was treated with potassium hydroxide for several days, degassed, and freshly distilled over sodium/benzophenone under nitrogen atmosphere. Styrene was passed through a neutral alumina column and then degassed before use. Isoprene was distilled under a nitrogen atmosphere. All chemicals were purchased from Sigma-Aldrich unless otherwise specified.

TG-MS measurements were performed using a Netzsch449 F3 Jupiter instrument under a dynamic Ar (99.999%) flow with a flow rate of 60 mL/min in a temperature range from 25 to 900 °C. A heating rate of 10 °C/min was used. About 5 mg of the sample was placed in an alumina (Al_2O_3) crucible. Simultaneous MS used a MS 403CAëolos with a detector secondary electron multiplier Chenneltron at a system pressure of 2×10^{-5} mbar. Gasses evolved under TG heat treatment were transferred to a MS detector using a quartz transfer capillary with an inside diameter of 75 μm that was heated to 220 °C. The upper limit of the MS detector was 100 amu. Raman spectroscopy was done using a Renishaw Raman RE01 microscopy with a 514.5 nm laser. The PF-GNRs were dispersed in *ortho*-dichlorobenzene using mild bath sonication (Cole-Parmer, EW-08849-00); the suspension was drop-cast onto Si chips with a 500 nm-thick SiO_2 layer, then the solvent was evaporated upon heating, and the sample was imaged using a JEOL 6500 field-emission microscope and 2100F field emission gun transmission electron microscope.

To prepare PF-GNRs, 0.1 g of alkali metal (Li, Na, or K), 0.256 g of naphthalene, and 50 mg of MWCNTs (Mitsui MWCNTs, NTL MWCNTs or Baytubes) were added to a 100 mL oven-dried Schlenk flask; 50 mL of THF was added. The flask was capped and the suspension was subjected to three freeze–pump–thaw cycles to remove oxygen. The reaction mixture was stirred at room temperature for 3 d, and 20 mL of monomer (styrene or isoprene) was added dropwise while the mixture was cooled in a dry ice/acetone bath. The mixture was stirred at room temperature for 1 d and then the reaction mixture was quenched by 20 mL of anhydrous ethanol. The gray precipitate was filtered through a polytetrafluoroethylene (PTFE) membrane (0.45 μm), followed by extraction with boiling chloroform in a Soxhlet extractor for 1 week to remove unbound polymer. The final product (55 mg of PF-GNRs) was collected on a PTFE membrane (0.45 μm), washed with THF (3×100 mL), ethanol (3×100 mL), DI water (3×100 mL), and acetone (50 mL) and ether (50 mL), and dried in vacuum oven at 60 °C overnight.

Conflict of Interest: The authors declare no competing financial interest.

Acknowledgment. We thank the Advanced Energy Consortium (BG Group, Halliburton, Conoco Phillips, BP, Shell, Total, Petrobras, Schlumberger), the AFOSR (FA9550-09-1-0581), Center of Excellence Low Carbon Technologies, Slovenia (CO NOT), Center of Excellence Advanced Materials and Technologies for the Future, Slovenia (CO NAMASTE), Sandia National Laboratory (1100745), the Lockheed Martin Corporation through the LANCER IV Program and the ONR MURI program (no. 00006766, N00014-09-1-1066) for funding. We thank A. Tanioka and M. Endo for the donation of the Mitsui MWCNTs, B. K. P. Hoelscher at MI SWACO for providing NTL MWCNTs, and H. Adams for donation of Baytubes.

Supporting Information Available: Synthesis, SEM, and TEM images and calculations. This material is available free of charge *via* the Internet at http://pubs.acs.org.

REFERENCES AND NOTES

1. Zhu, Y.; James, D. K.; Tour, J. M. New Routes to Graphene, Graphene Oxide and Their Related Applications. *Adv. Mater.* **2012**, *24*, 4924–4955.
2. Kosynkin, D. V.; Higginbotham, A. L.; Sinitskii, A.; Lomeda, J. R.; Dimiev, A.; Price, B. K.; Tour, J. M. Longitudinal Unzipping of Carbon Nanotubes To Form Graphene Nanoribbons. *Nature* **2009**, *458*, 872–876.
3. Cano-Márquez, A. G.; Rodríguez-Macías, F. J.; Campos-Delgado, J.; Espinosa-González, C. G.; Tristán-López, F.; Ramírez-González, D.; Cullen, D. A; Smith, D. J.; Terrones, M.; Vega-Cantú, Y. I. Ex-MWNTs: Graphene Sheets and Ribbons Produced by Lithium Intercalation and Exfoliation of Carbon Nanotubes. *Nano Lett.* **2009**, *9*, 1527–1533.
4. Elías, A. L.; Botello-Méndez, A. R.; Meneses-Rodríguez, D.; Jehová González, V.; Ramírez-González, D.; Ci, L.; Muñoz-Sandoval, E.; Ajayan, P. M.; Terrones, H.; Terrones, M. Longitudinal Cutting of Pure and Doped Carbon Nanotubes to Form Graphitic Nanoribbons Using Metal Clusters as Nanoscalpels. *Nano Lett.* **2010**, *10*, 366–372.
5. Kosynkin, D. V.; Lu, W.; Sinitskii, A.; Pera, G.; Sun, Z.; Tour, J. M. Highly Conductive Graphene Nanoribbons by Longitudinal Splitting of Carbon Nanotubes Using Potassium Vapor. *ACS Nano* **2011**, *5*, 968–974.
6. Genorio, B.; Lu, W.; Dimiev, A. M.; Zhu, Y.; Raji, A.-R. O.; Novosel, B.; Alemany, L. B.; Tour, J. M. *In Situ* Intercalation Replacement and Selective Functionalization of Graphene Nanoribbon Stacks. *ACS Nano* **2012**, *6*, 4231–4240.
7. Morelos-Gómez, A.; Vega-Díaz, S. M.; González, V. J.; Tristán-López, F.; Cruz-Silva, R.; Fujisawa, K.; Muramatsu, H.; Hayashi, T.; Mi, X.; Shi, Y.; *et al.* Clean Nanotube Unzipping by Abrupt Thermal Expansion of Molecular Nitrogen: Graphene Nanoribbons with Atomically Smooth Edges. *ACS Nano* **2012**, *6*, 2261–2272.
8. Kaisersberger, E. Combined Thermal Analysis and Gas-Analysis Methods and Software Simulations for the Investigation of the Potential Endangerment to the Environment through Production and Recycling Processes. *Thermochim. Acta* **1999**, *101*, 267–234.
9. For the degradation products of polystyrene, see http://webbook.nist.gov/cgi/cbook.cgi?ID=C100425&Units=SI&Mask=608#Mass-Spec (accessed November 13, 2012).
10. Ferrari, A. C.; Robertson, J. Interpretation of Raman Spectra of Disordered and Amorphous carbon. *Phys. Rev. B* **2000**, *61*, 14095–14107.
11. R. Vidano, D. B. F. New Lines in the Raman Spectra of Carbons and Graphite. *J. Am. Ceram. Soc.* **1978**, *61*, 13–17.
12. Campos-Delgado, J.; Romo-Herrera, J. M.; Jia, X.; Cullen, D. A; Muramatsu, H.; Kim, Y. A.; Hayashi, T.; Ren, Z.; Smith, D. J.; Okuno, Y.; *et al.* Bulk Production of a New Form of sp^2 Carbon: Crystalline Graphene Nanoribbons. *Nano Lett.* **2008**, *8*, 2773–2778.
13. Solin, S. A. Raman and IR Studies of Intercalated Graphite. *Physica* **1980**, *99B*, 443–453.
14. Inagaki, M.; Tanaike, O. Host Effect on the Formation of Sodium-Tetrahydrofuran-Graphite. *Synth. Met.* **1995**, *73*, 77–81.
15. Shih, C.-J.; Vijayaraghavan, A.; Krishnan, R.; Sharma, R.; Han, J.-H.; Ham, M.-H.; Jin, Z.; Lin, S.; Paulus, G. L. C.; Reuel, N. F.; *et al.* Bi- and Trilayer Graphene Solutions. *Nat. Nanotechnol.* **2011**, *6*, 439–445.
16. Englert, J. M.; Dotzer, C.; Yang, G.; Schmid, M.; Papp, C.; Spiecker, E.; Hauke, F.; Hirsch, A.; Gottfried, J. M.; Steinru, H. Covalent Bulk Functionalization of Graphene. *Nat. Chem.* **2011**, *3*, 279–286.
17. Mordkovich, V. Z.; Baxendaleg, M.; Yoshjmura, S.; Chang, R. P. H. Intercalation into Carbon Nanotubes. *Carbon* **1996**, *34*, 1301–1303.
18. Endo, M.; Saito, R.; Dresselhaus, M. S.; Dresselhaus, G. *Carbon Nanotubes: Preparation and Properties*; Ebbesen, T. W., Ed.; CRC Press: Boca Raton, FL, 1997; p 69.
19. Nakamizo, M.; Kammereck, R.; Walker, P. J. J. Laser Studies on Carbons. *Carbon* **1974**, *12*, 259–267.
20. Voiry, D.; Vallés, C.; Roubeau, O.; Pénicaud, A. Dissolution and Alkylation of Industrially Produced Multiwalled Carbon Nanotubes. *Carbon* **2011**, *49*, 170–175.
21. Forsman, W. C.; Dziemianowicz, T.; Leong, K.; Carl, D. Graphite Intercalation Chemistry: An Interpretive Review. *Synth. Met.* **1983**, *5*, 77–100.
22. Yu, M.; Lourie, O.; Dyer, M. J.; Moloni, K.; Kelly, T. F.; Ruoff, R. S. Strength and Breaking Mechanism of Multiwalled Carbon Nanotubes Under Tensile Load. *Science* **2000**, *287*, 637–640.